23PM3E-07

Exact Absorbing Boundary Conditions for Numerical Modeling of 3-D Diffraction Gratings

Kostyantyn Sirenko [#1], Yuriy Sirenko [*2], Hakan Bagci [#3]

[#] *King Abdullah University of Science and Technology (KAUST)*
4700 KAUST, Thuwal, 23955, Saudi Arabia
[1] kostyantyn.sirenko@kaust.edu.sa
[3] hakan.bagci@kaust.edu.sa

[*] *Institute of Radiophysics and Electronics of National Academy of Sciences of Ukraine (IRE NASU)*
12 Acad. Proskura str., Kharkiv, 61085, Ukraine
[2] yks@ire.kharkov.ua

Abstract—**Exact absorbing boundary conditions (EACs) for highly-accurate modeling of transient electromagnetic waves interaction on 3-D diffraction gratings are rigorously derived. EACs when enforced together with periodic boundary conditions permit the truncation of the infinite physical domain of the gratings to a bounded computation domain without introducing any additional errors. Numerical results demonstrate that discretization error of the EACs matches the error of the method used of discretizing the Maxwell equations, and therefore suggest that EAC-based truncation might result in more accurate or efficient simulations when compared to PML-based truncation.**

I. Introduction

Increasing geometrical complexity of modern electronic and optical devices has rendered simulation tools, which are capable of accurately computing electromagnetic interactions on three-dimensional (3-D) geometric models, indispensible. Simulation tools specifically developed for diffraction gratings are no different. Classical mathematical models of diffraction gratings, which have been developed within the last forty years, are mostly two-dimensional (2-D) models and do not account for field variations in all three dimensions [1], [2]. Additionally, time domain models/simulation tools are often preferred over their frequency-domain counterparts. This is mostly motivated by the fact that time domain simulators allow for real-time observation of physical phenomena, can account for nonlinear medium components or medium parameters, and provide broadband results with a single code execution. As a result, 3-D differential equation based time domain methods, including finite difference time domain (FDTD) method and finite element methods (FEM) have become popular in simulation of transient electromagnetic interactions on diffraction gratings.

It is well known that application of a differential equation based method in a problem with an unbounded physical domain requires the domain to be truncated. The most widespread truncation method is to wrap the domain of interest with layers of specially designed absorbing/lossy material, so called perfectly matched layers (PMLs) [3], [4]. Although PML truncation is easy to formulate/implement and error-controllable up to certain degree, it might induce non-negligible errors in the solution especially during the simulation of long-duration processes [5].

In this work, derivation of a set of exact absorbing boundary conditions (EACs) for accurately truncating unbounded physical domains is provided. The presented EACs rigorously derived from the radiation conditions for outgoing waves [2], [5]–[8]. These EACs, when enforced together with periodic boundary conditions, permit highly accurate characterization of transient electromagnetic interactions on 3-D diffraction gratings. The EACs are implemented within a higher order time domain discontinuous Galerkin finite element (TD-DG-FEM) framework [4], [5], [9].

Numerical results demonstrate that discretization error of the EACs matches the error of TD-DG-FEM for various orders of interpolation functions used in the discretization, and therefore suggest that EAC-based truncation might result in more accurate or efficient simulations when compared to PML-based truncation.

II. Problem Formulation

Let Ω represent domain of the unit cell of the 3-D diffraction grating. Ω is assumed to extend to infinity along the z direction while it is terminated at $x = l_x$ and $y = l_y$ (Fig.1). The (unbounded) domain of the diffraction grating is generated by replicating Ω with periods l_x and l_y in x and y directions, respectively. The grating profile is determined by material parameters, namely, relative permittivity $\varepsilon(\mathbf{r})$ and relative permeability $\mu(\mathbf{r})$, $\mathbf{r} = (x, y, z) \in \mathbb{R}^3$. As expected, the same assumption of periodicity applies to $\varepsilon(\mathbf{r})$ and $\mu(\mathbf{r})$:

$$\begin{aligned} \varepsilon(x + l_x, y + l_y, z) &= \varepsilon(x, y, z) \\ \mu(x + l_x, y + l_y, z) &= \mu(x, y, z) \end{aligned} \tag{1}$$

For simplicity of description of the formulation, it is assumed that the grating is excited by a normally incident plane wave. Under this assumption, time-dependent electric and magnetic fields, $\mathbf{E}(\mathbf{r}, t)$ and $\mathbf{H}(\mathbf{r}, t)$, posses the same periodic properties as $\varepsilon(\mathbf{r})$ and $\mu(\mathbf{r})$:

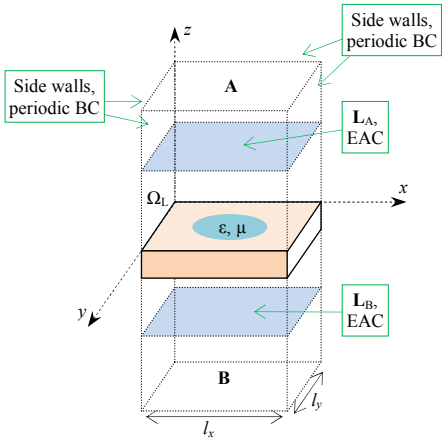

Fig. 1. Unit cell, Ω, of 3-D diffraction grating

$$\begin{aligned}\mathbf{E}(x+l_x,y+l_y,z,t)&=\mathbf{E}(x,y,z,t)\\ \mathbf{H}(x+l_x,y+l_y,z,t)&=\mathbf{H}(x,y,z,t).\end{aligned}\tag{2}$$

In this work, it is assumed that $\mathbf{E}(\mathbf{r},t)$ and $\mathbf{H}(\mathbf{r},t)$ are governed by the unit-free normalized Maxwell equations [4], [5], [9]. To find the fields $\mathbf{E}(\mathbf{r},t)$ and $\mathbf{H}(\mathbf{r},t)$ on the grating numerically, the unbounded physical domain should be truncated to a bounded computation domain. Truncations in x and y directions and z direction are achieved by imposing the periodic boundary conditions (2) on the side walls of Ω and EACs on the virtual boundaries $\mathbf{L}_A$ and $\mathbf{L}_B$, respectively (Fig. 1). This operation reduces the physical domain $\mathbb{R}^3$ to the computation domain denoted by Ω_L (Fig.1). Note this truncation is mathematically rigorous and does not involve any approximations as detailed in the next section.

III. Exact Absorbing Boundary Conditions

The derivation of EACs enforced on the virtual boundaries $\mathbf{L}_A$ and $\mathbf{L}_B$ follows the standard mathematical steps described in [2], [6]–[8]. Since the derivation of EAC on $\mathbf{L}_B$ is same as that on $\mathbf{L}_A$, only the derivation of the EAC on $\mathbf{L}_A$ is provided in what follows. In the homogeneous external region **A** (Fig. 1), fields $\mathbf{E}(\mathbf{r},t)$ and $\mathbf{H}(\mathbf{r},t)$ satisfy the homogeneous wave equation:

$$\begin{aligned}&\partial_t^2\mathbf{U}(\mathbf{r},t)=\partial_x^2\mathbf{U}(\mathbf{r},t)+\partial_y^2\mathbf{U}(\mathbf{r},t)+\partial_z^2\mathbf{U}(\mathbf{r},t),\quad t>0\\ &\mathbf{U}(\mathbf{r},0)=\partial_t\mathbf{U}(\mathbf{r},t)\big|_{t=0}=0.\end{aligned}\tag{3}$$

Here, $\mathbf{r}\in\mathbf{A}\bigcup\mathbf{L}_A$, $\mathbf{U}(\mathbf{r},t)\in\{\mathbf{E}(\mathbf{r},t),\mathbf{H}(\mathbf{r},t)\}$. Solution of (3), $\mathbf{U}(\mathbf{r},t)$, is expanded in terms of modes using the separation of variables:

$$\mathbf{U}(\mathbf{r},t)=\sum_{n=-\infty}^{\infty}\sum_{m=-\infty}^{\infty}\mathbf{u}_{nm}(z,t)\psi_{nm}(x,y).\tag{4}$$

Here, $\mathbf{u}_{nm}(z,t)$ are unknown spatio-temporal amplitudes; $\psi_{nm}(x,y)$ are transverse eigenfunctions. Orthogonality of the eigenfunctions yields a relation between $\mathbf{u}_{nm}(z,t)$ and $\mathbf{U}(\mathbf{r},t)$:

$$\mathbf{u}_{nm}(z,t)=\int_0^{l_x}\int_0^{l_y}\mathbf{U}(\mathbf{r},t)\,\psi_{nm}(x,y)\,dxdy.\tag{5}$$

The transverse eigenfunctions $\psi_{nm}(x,y)$ and the corresponding eigenvalues λ_{nm} are non-trivial solutions of the homogeneous problem

$$\begin{aligned}&\partial_x^2\psi_{nm}(x,y)+\partial_y^2\psi_{nm}(x,y)+\lambda_{nm}^2\psi_{nm}(x,y)=0,\\ &\begin{Bmatrix}\psi_{nm}\\ \partial_x\psi_{nm}\end{Bmatrix}(l_x,y)=\begin{Bmatrix}\psi_{nm}\\ \partial_x\psi_{nm}\end{Bmatrix}(0,y),\\ &\begin{Bmatrix}\psi_{nm}\\ \partial_y\psi_{nm}\end{Bmatrix}(x,l_y)=\begin{Bmatrix}\psi_{nm}\\ \partial_y\psi_{nm}\end{Bmatrix}(x,0),\\ &0\le x<l_x,\quad 0\le y<l_y.\end{aligned}\tag{6}$$

The problem (6) can be easily solved:

$$\begin{aligned}&\alpha_n=2\pi n/l_x,\ \beta_m=2\pi m/l_y,\ \lambda_{nm}^2=\alpha_n^2+\beta_m^2;\\ &n\ge0,\ m\ge0:\ \psi_{nm}(x,y)=(l_xl_y)^{-1/2}\cos(\alpha_nx)\cos(\beta_my),\\ &n\ge0,\ m<0:\ \psi_{nm}(x,y)=(l_xl_y)^{-1/2}\cos(\alpha_nx)\sin(\beta_my),\\ &n<0,\ m\ge0:\ \psi_{nm}(x,y)=(l_xl_y)^{-1/2}\sin(\alpha_nx)\cos(\beta_my),\\ &n<0,\ m<0:\ \psi_{nm}(x,y)=(l_xl_y)^{-1/2}\sin(\alpha_nx)\sin(\beta_my),\\ &0\le x<l_x,\ 0\le y<l_y.\end{aligned}$$

The amplitudes $\mathbf{u}_{nm}(z,t)$ are solutions of the initial value problem

$$\begin{aligned}&-\partial_t^2\mathbf{u}_{nm}(z,t)+\partial_z^2\mathbf{u}_{nm}(z,t)-\lambda_{nm}^2\mathbf{u}_{nm}(z,t)=0,\quad z\ge l_A,\ t>0\\ &\mathbf{u}_{nm}(z,0)=\partial_t\mathbf{u}_{nm}(z,t)\big|_{t=0}=0,\ z\ge l_A.\end{aligned}\tag{7}$$

Initial value problem (7) can be solved analytically in the spectral domain. Applying cosine Fourier transform with respect to z to (7) yields:

$$\begin{aligned}&\partial_t^2\tilde{\mathbf{u}}_{nm}(\omega,t)+(\lambda_{n,m}^2+\omega^2)\tilde{\mathbf{u}}_{nm}(\omega,t)=\\ &-(2/\pi)^{1/2}\,\partial_z\mathbf{u}_{nm}(z,t)\big|_{z=l_A},\ \omega>0,\ -\infty<t<\infty.\end{aligned}\tag{8}$$

Here, $\tilde{\mathbf{u}}_{nm}(\omega,t)$ is the cosine Fourier transform of $\mathbf{u}_{nm}(z,t)$. Equation (8) describes a generalized Cauchy problem for $\tilde{\mathbf{u}}_{nm}(\omega,t)$ [6]–[8]. The fundamental solution of the operator in left-hand side of (8) is given by $F(t)=\chi(t)G(t)$,where $G(t)=(\lambda_{nm}^2+\omega^2)^{-1/2}\sin[t(\lambda_{nm}^2+\omega^2)^{1/2}]$ and $\chi(t)$ is the Heaviside step function [6]–[8]. Then, the solution of (8) is obtained by convolving $F(t)$ with its right-hand side:

$$\tilde{\mathbf{u}}_{nm}(\omega,t)=-(2/\pi)^{1/2}\int_0^t G(t-\tau)\partial_z\mathbf{u}_{nm}(z,\tau)\big|_{z=l_A}\,d\tau,\ t\ge0.\tag{9}$$

Applying the inverse cosine Fourier transform to (9) and evaluating the resulting expression at $z=l_A$ yields:

$$\mathbf{u}_{nm}(l_A,t)=-\int_0^t J_0\left[(t-\tau)\lambda_{nm}\right]\partial_z\mathbf{u}_{nm}(z,\tau)\big|_{z=l_A}\,d\tau.\tag{10}$$

where $J_0(.)$ is the zeroth order Bessel function. Differentiating (10) with respect to t, taking the Laplace transform of the resulting equation followed by several rearrangements in the Laplace domain, and finally applying the inverse Laplace transform, one can obtain [6], [8]:

$$\partial_t \mathbf{u}_{nm}(l_A,t)+\partial_z \mathbf{u}_{nm}(z,t)\big|_{z=l_A}=\lambda_{nm}\int_0^t K(t-\tau)\mathbf{u}_{nm}(l_A,\tau)\,d\tau. \quad (11)$$

where $K(t)=-J_1(t\lambda_{nm})/t$ and $J_1(.)$ is the first order Bessel function. Using (4) and (5) in (11), yields a relation between $\mathbf{U}(\mathbf{r},t)$ and its spatial and temporal derivatives evaluated on the virtual boundary $\mathbf{L}_A$:

$$\partial_t \mathbf{U}(\mathbf{r}_A,t)+\partial_z \mathbf{U}(\mathbf{r},t)\big|_{\mathbf{r}=\mathbf{r}_A}=\sum_{n=-\infty}^{\infty}\sum_{m=-\infty}^{\infty}\lambda_{nm}\psi_{nm}(x,y) \times\int_0^t K(t-\tau)\int_0^{l_x}\int_0^{l_y}\mathbf{U}(\tilde{\mathbf{r}}_A,t)\,\psi_{nm}(\tilde{x},\tilde{y})\,d\tilde{x}d\tilde{y}d\tau. \quad (12)$$

Here, $\mathbf{r}_A=(x,y,l_A)$ and $\tilde{\mathbf{r}}_A=(\tilde{x},\tilde{y},l_A)$ are points on the virtual boundary $\mathbf{L}_A$; $0\le x<l_x$, $0\le y<l_y$, and $t\ge 0$. Following the same mathematical steps, one can obtain the EAC enforced for $\mathbf{U}(\mathbf{r},t)$ on the virtual boundary $\mathbf{L}_B$:

$$\partial_t \mathbf{U}(\mathbf{r}_B,t)-\partial_z \mathbf{U}(\mathbf{r},t)\big|_{\mathbf{r}=\mathbf{r}_B}=\sum_{n=-\infty}^{\infty}\sum_{m=-\infty}^{\infty}\lambda_{nm}\psi_{nm}(x,y) \times\int_0^t K(t-\tau)\int_0^{l_x}\int_0^{l_y}\mathbf{U}(\tilde{\mathbf{r}}_B,t)\,\psi_{nm}(\tilde{x},\tilde{y})\,d\tilde{x}d\tilde{y}d\tau. \quad (13)$$

Here, $\mathbf{r}_B=(x,y,l_B)$ and $\tilde{\mathbf{r}}_B=(\tilde{x},\tilde{y},l_B)$ are points on the virtual boundary $\mathbf{L}_B$; $0\le x<l_x$, $0\le y<l_y$, and $t\ge 0$.

Equations (12) and (13) establish the relations between the electromagnetic fields $\mathbf{E}(\mathbf{r},t)$ and $\mathbf{H}(\mathbf{r},t)$ and their temporal and spatial derivatives evaluated on the virtual boundaries $\mathbf{L}_A$ and $\mathbf{L}_B$. Thus, they can be used as EACs: $\mathbf{E}(\mathbf{r},t)$ and $\mathbf{H}(\mathbf{r},t)$, which originate in Ω_L and arrive onto $\mathbf{L}_A$ and $\mathbf{L}_B$ are neither deformed nor reflected back into Ω_L; they act as if they are being absorbed by the regions **A** and **B** (or by the virtual boundaries $\mathbf{L}_A$ and $\mathbf{L}_B$). If EACs are discretized using a scheme that has the same accuracy of the method used for discretizing Maxwell equations in Ω_L, they do not introduce any additional errors into numerical solution. It should be noted here that the EACs (12) and (13) are more suitable to be discretized within TD-DG-FEM [5]. Through mathematical manipulation [6]-[8], this form of the EACs can be converted into a form that can be easily discretized by FDTD [7].

IV. Numerical Results

The EACs derived in Section III are implemented in a high-order TD-DG-FEM [4], [5], [9]. The accuracy of the EAC implementation is demonstrated by numerical simulation of a reflective grating that is excited by a normally incident plane wave. The error of EAC domain truncation is compared with the errors of the PML [4] and the first-order ABC [5] truncations implemented within the same TD-DG-FEM.

The grating profile of the unit cell is a perfect electrically conducting (PEC) truncated pyramid centered on a plane substrate (Fig 2). The lengths of pyramid's edges at the bottom and the top bases, and its height are $a=0.42$ and $b=0.28$, and $h=0.5$, respectively. The grating's period in x and y directions is the same: $l_x=l_y=0.5$. The computation domain in the case of EAC truncation is $\Omega_L=[0\,;0.5]\times[0\,;0.5]\times[0\,;2]$ and the virtual boundary $\mathbf{L}_A$ with EAC (12) is located at $l_A=2$. Ω_L is discretized using a tetrahedral mesh with an average element size of 0.1. This discretization results in 3357 elements. The number of harmonics used in expansion (4) is 5: $n,m=0,\ \pm1,\ \pm2$. The first-order ABC truncation is applied in the same computation domain used by the EAC truncation, i.e., it is enforced at $z=l_A=2$. PML truncation is located beyond $z=2$; two PML truncations with thickness 0.25 and 0.5 are tested.

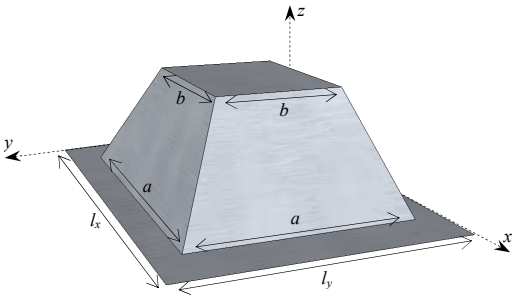

Fig. 2. Geometry of the pyramidal grating.

The excitation is introduced using total field/scattered field (TF/SF) technique [4], [5]. The TF/SF boundary is located at $z=1.5$, the non-zero components of incident plane wave are $H_x^{\text{in}}(x,y,-1.5,t)=E_y^{\text{in}}(x,y,-1.5,t)=e^{-(t-t_0)^2/4\alpha^2}\cos(\kappa(t-t_0))$, where $t_0=1.5$ is the delay, $\alpha=0.18$ is the measure of duration, and $\kappa=15$ is the modulation frequency. The total duration of simulation is 7.5, which is long enough to allow the incident wave to be reflected by the grating and then pass through the virtual boundary with absorbing condition.

As a measure of accuracy the global relative L^2-error is used:

$$err_{\text{rel}}(t)=\sqrt{\int_{\Omega_{err}}\left|E_y(\mathbf{r},t)-E_y^{ref}(\mathbf{r},t)\right|^2 d\mathbf{r}\Big/\int_{\Omega_{err}}\left|E_y^{ref}(\mathbf{r},t)\right|^2 d\mathbf{r}}\,.$$

Here, Ω_{err} coincides with the EAC-truncated computation domain Ω_L and $E_y^{ref}(\mathbf{r},t)$ and $E_y(\mathbf{r},t)$ are obtained by the TD-DG-FEM using PEC boundary condition and EAC, ABC, or PML truncations, respectively. During the computation of $E_y^{ref}(\mathbf{r},t)$ the PEC boundary condition is enforced at $z=6$, i.e, the reference computation domain $\Omega_{ref}=[0\,;0.5]\times[0\,;0.5]\times[0\,;6]$. Note that Ω_{ref} is large enough to prevent reflections coming back into the domain of interest Ω_{err} within the duration of simulation. This definition of accuracy takes into account only the error caused by the domain truncation and is independent of the error of the method used for discretizing the Maxwell equations.

Fig. 3 plots errors computed at the end of the simulations, $err_{\text{rel}}(7.5)$, against the order of interpolation polynomials, p, used in the TD-DG-FEM discretization as well as the discretization of the EAC and the ABC. It is clearly seen that error of the EAC truncation decreases with the growing polynomial order, while the errors of the ABC and the PML truncations remain virtually the same for any polynomial order. This clearly indicates that the accuracy of the EAC truncation naturally matches the overall accuracy of numerical method (set by the polynomial order, p). The overall accuracy of simulations with the ABC or PML truncations is limited by the accuracy of truncating equation and increasing the polynomial order does not result in more accurate results.

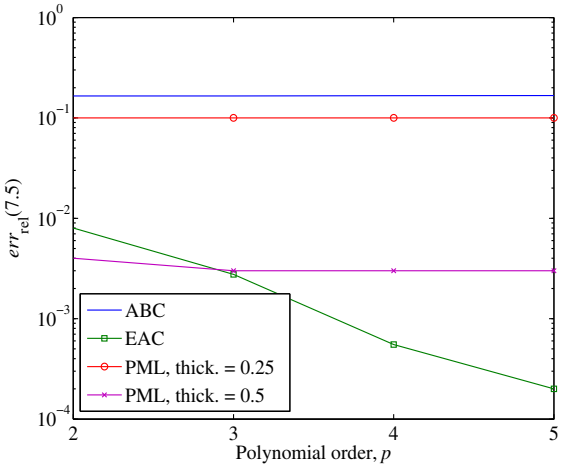

Fig. 3. Related errors at the end of simulations, $err_{rel}(7.5)$.

V. Conclusion

The paper details the mathematical derivation of EACs that are used together with periodic boundary conditions to truncate the physical domains in time domain simulations of 3-D diffraction gratings. It is demonstrated that EACs, when properly discretized, does not introduce any additional errors to the solution and are superior to more widespread domain truncation techniques making use of PML and ABCs in terms of accuracy especially when a higher order scheme is used to discretize the Maxwell equations.

References

[1] M. Neviere and E. Popov, *Light Propagation in Periodic Media: Differential Theory and Design*. New York, USA: Marcel Dekker, 2003.

[2] Y. K. Sirenko and S. Strom, Ed., *Modern Theory of Gratings. Resonant Scattering: Analysis Techniques and Phenomena*. Berlin, Germany: Springer, 2010.

[3] E. Turkel and A. Yefet, "Absorbing PML boundary layers for wave-like equations," *Appl. Numer. Math.*, vol. 27, pp. 533–557, 1998.

[4] M. Liu, K. Sirenko, and H. Bagci, "An efficient discontinuous Galerkin finite element method for highly accurate solution of Maxwell equations," *IEEE Trans. Antennas Propagat.*, vol. 60, no. 8, pp. 3992–2998, Aug. 2012.

[5] K. Sirenko, M. Liu, and H. Bagci, "Incorporation of exact boundary conditions into a discontinuous Galerkin finite element method for accurately solving 2D time-dependent Maxwell equations," *IEEE Trans. Antennas Propagat.*, DOI 10.1109/TAP.2012.2220102, in press, to appear in vol. 61, no. 1, Jan. 2013.

[6] K. Y. Sirenko, Y. K. Sirenko, and N. P. Yashina, "Modeling and analysis of transients in periodic gratings. I. Fully absorbing boundaries for 2-D open problems," *J. Opt. Soc. Am. A*, vol. 27, pp. 532–543, 2010.

[7] K. Sirenko, V. Pazynin, Y. K. Sirenko, and H. Bagci, "An FFT-accelerated FDTD scheme with exact absorbing conditions for characterizing axially symmetric resonant structures," *Progress in Electromagnetics Research*, vol. 111, pp. 331–364, 2011.

[8] Y. K. Sirenko, S. Strom, and N. P. Yashina, *Modeling and Analysis of Transient Processes in Open Resonant Structures. New Methods and Techniques*. Berlin, Germany: Springer 2007.

[9] J. S. Hesthaven and T. Warburton, *Nodal Discontinuous Galerkin Methods.* New York, USA: Springer, 2008.